



DIGITAL ACCESS TO SCHOLARSHIP AT HARVARD

Integrated Circuit / Microfluidic Chips for Dielectric Manipulation

The Harvard community has made this article openly available.
[Please share](#) how this access benefits you. Your story matters.

Citation	Hunt, Thomas P., David Issadore, Keith Andrew Brown, Hakho Lee and Robert M. Westervelt. 2009. Integrated circuit / microfluidic chips for dielectric manipulation. In Lab on a chip technology: Biomolecular separation and analysis, ed. K. E. Herold and A. Rasooly. Norfolk, UK: Caister Academic Press.
Accessed	February 18, 2015 4:31:16 PM EST
Citable Link	http://nrs.harvard.edu/urn-3:HUL.InstRepos:4239030
Terms of Use	This article was downloaded from Harvard University's DASH repository, and is made available under the terms and conditions applicable to Other Posted Material, as set forth at http://nrs.harvard.edu/urn-3:HUL.InstRepos:dash.current.terms-of-use#LAA

(Article begins on next page)

Integrated Circuit / Microfluidic Chips for Dielectric Manipulation

Thomas P. Hunt^{2,3}, D. Issadore¹, K.A. Brown¹, Hakho Lee^{1,4}, and R.M. Westervelt^{1,2}

1. School of Engineering & Applied Sciences, Harvard University, Cambridge MA 02138.
2. Dept of Physics, Harvard University, Cambridge, MA 02138.
3. Present address: Dept of Bioengineering, University of California, Berkeley, 94720.
4. Present address: Center for Molecular Imaging Research, Massachusetts General Hospital, Harvard Medical School, Charlestown, MA 02130.

Abstract

In this chapter, we describe the development of Integrated-Circuit/Microfluidic chips that can move individual living cells and chemical droplets along programmable paths using dielectrophoresis (DEP). These hybrid chips combine the biocompatibility of a microfluidic system with the complexity and programmability of an integrated circuit (IC) - a microfluidic chamber is built directly on top of the IC - and they offer new opportunities for sensing, actuation, and control. IC/Microfluidic chips can independently control the location of hundreds of dielectric objects, such as biological cells or chemical droplets, in the microfluidic chamber at the same time. The IC couples with suspended objects by using spatially patterned, time-dependent electromagnetic fields. The IC layout is similar to a computer display: it consists of a two-dimensional array of 128x256 metal 'pixels', each 11x11 μm^2 in size, controlled by a built-in SRAM memory. Each pixel can be energized by a radio frequency (RF) voltage up to 5 V_{pp} . The ICs were made in a commercial foundry, and a microfluidic chamber was built on its top surface at Harvard. Using this IC/Microfluidic chip, we have moved yeast and mammalian cells

along programmed paths at speeds up to 300 $\mu\text{m}/\text{sec}$. Hundreds of cells can be individually trapped and simultaneously positioned into controlled patterns. The chip can trap and move pL droplets of water in oil, split one droplet into two, and mix two droplets into one, allowing one to conduct experiments with chemicals and individual cells, using tiny amounts of fluid. Our IC/Microfluidic chip provides a programmable platform that can individually control the motion of large numbers of cells and fluid droplets simultaneously for lab-on-a-chip applications.

Section 1. Introduction

1.1 Motivation and Background

Fields such as drug discovery, genetic sequencing and synthesis, and cell sorting demand fast and efficient manipulation of increasingly large numbers of decreasingly small volumes of fluids. The burgeoning field of microfluidics has produced a library of miniaturized tools to interact with biological objects and sub-microliter fluid samples on the length scale of single cells. Tools such as valves, pipes, and mixers have been fabricated in materials such as glass, silicon, and inexpensive polymer molds to control fluids on the micrometer scale (Whitesides et al., 2001, Stone et al., 2005, Tabeling et al., 2005). A micrograph of polymer microfluidic channels made with a commonly used polymer called PDMS is shown in Figure 1a.

The paradigm shift in fluid handling from large, single purpose equipment to miniaturized tools that can be integrated into small, complex, and cheap laboratories-on-a-chip, is analagous to what was faced by the semiconductor industry half of a century ago and which led to the integrated circuit (IC) (Throsen et al., 2002, Lee et al., 2007). Electronic circuits fifty years ago were built from discrete elements and could perform specific tasks. These simple circuits eventually gave way to integrated circuits and eventually

microprocessors that could be programmed to execute many different tasks and are now ubiquitously found as the brains of modern technology. An example of a modern integrated circuit, the Intel Dual Core processor, is shown in Figure 1c. We envision that integrated circuits coupled with miniature fluid handling elements will open up many possibilities for fluidic systems. Microfluidic devices have been built for many specific biological experiments; one impressive recent example is a fully integrated on-chip DNA sequencer (Blazej et al., 2006). Pneumatically actuated programmable microfluidic systems are currently being developed to meet the demand for complex fluid manipulation, as is shown in Figure 1b (Squires et al., 2005).

Discrete electronics has been combined with microfluidics to provide enhanced capabilities such as programmable fluid handling, chemical and biological sensing, control logic and memory that can respond to external stimuli, and the ability to analyze and report the results of experiments to the outside world (Lee et al., 2007). Hybrid IC/Microfluidic systems have been developed in which the fluidics are built directly on top of integrated circuits offering unprecedented sensing and actuation (Figure 1d).

An integrated circuit with hundreds of millions of transistors connected by a complex network of wires can be inexpensively mass-produced on a silicon chip. Devices on a chip are capable of detecting and producing electric and magnetic fields, heat, and light, providing a variety of ways to probe and sense objects nearby. GHz switching speeds can be easily achieved. The steady miniaturization of circuit elements since the invention of the IC has made it possible to produce a chip such as in the Intel Dual Core processor (Figure 1c) which has nearly one billion transistors, made using a 45 nm process. To sense the spatial scale of devices on ICs, consider that > 1000 transistors fit in the $10 \times 10 \mu\text{m}^2$ area beneath a single cell, or below

a pL droplet. It is remarkable that ICs with these characteristics can be inexpensively mass produced, at costs of a few dollars per chip.

Integrated circuits interact with fluids and biological samples by generating and sensing electric and magnetic fields. Nano-particles (Green et al., 1997, Cohen et al., 2005), cells (Pohl et al., 1966, Manaresi et al., 2003), molecules (Han et al., 1995, Cohen et al., 2005), and fluid samples (Cho et al., 2003, Hunt et al., 2008) have been trapped, moved, and sorted with micro-patterned electric fields using dielectrophoresis (Pohl et al., 1966, Green et al., 1997, Manaresi et al., 2003, Hunt et al., 2008), electrophoresis (Cohen et al., 2005), electro-osmosis (Cohen et al., 2005), and electro-wetting (Cho et al., 2005). Likewise, magnetic nanoparticles attached to biological samples have been trapped and moved (Lee et al., 2003), and sorted with magnetic fields (Inglis et al., 2004, Xia et al., 2006, Lee et al., 2007).

In addition to moving and sorting objects, integrated circuits have been used to sense nanoparticles, cells, and fluids. One modality is to electrically sense objects' response to applied electric fields. Dielectric spectroscopy (Poloveya et al., 1999, Facer et al., 2001) and capacitive sensing (Wood, 2005) of biological fluids (Facer et al., 2001), nano-particles (Wood, 2005), and cells (Poloveya, 2001) has been demonstrated. In addition, electric fields can be used for recording and stimulating electrogenic cells (DeBusschere et al., 2001, Eversmann et al., 2003).

Magnetic sensing has been used to carry out nuclear magnetic resonance (NMR) measurements of fluids and biological objects. Systems for NMR spectroscopy have been miniaturized (Maguire et al., 2007) and a hand-held system for small-scale T2 relaxometry has been developed (Yong et al., 2008). Additionally, optical systems have been integrated with microfluidic and electrical systems for low-cost colorimetric (Chin et al., 2007), fluorescence (Psaltis et al., 2006), and nanoparticle sensing (Psaltis et al., 2006, Chin et al., 2007).

IC/Microfluidic chips offer the possibility to control single suspended cells and pL droplets of fluids; sensing and actuation can be tied together in a feedback loop to make smart chips for biomedical applications. Moving a small object in a microfluidic chamber requires times ~ 1 msec or more. This allows a chip operating on a GHz clock to run many computations during each actuation cycle. IC/Microfluidics chips can be made with areas ($\sim 1 \text{ cm}^2$) large enough to sense and control the motion of hundreds of cells or droplets on a single chip at the same time.

The hybrid IC/Microfluidic chip that we describe here uses dielectrophoresis (DEP) to manipulate cells and droplets. Dielectrophoresis, the motion of a dielectric object caused by changes in electric field magnitude, provides a versatile manipulation scheme that is well suited to microfluidic systems. By using a spatially patterned electric field, one can apply a force to any object that has a dielectric constant different than the surrounding liquid with DEP. Most DEP systems rely on a small number of electrodes to perform a set task. Dielectrophoresis has been used to move cells (Pohl and Crane, 1971), nanoparticles (Green and Morgan, 1997), viruses (Green et al., 1997), and single molecules (Hölzel et al., 2005), as well as to sort droplets (Ahn et al., 2006).

Our vision is to replace the small set of single-purpose electrodes in a dedicated DEP system with a large two-dimensional array of programmable pixels in an integrated circuit. Objects to be manipulated are contained in a microfluidic chamber just above the chip's surface, and they are observed using an optical microscope. The pixel array creates a spatial 'image' of electric field intensity in the microfluidic chamber, like a computer display creates an optical image. Objects with large dielectric constant ϵ are attracted toward electric field peaks, while objects with small ϵ are pulled toward minima. As the process proceeds, the electric field 'image'

and the forces it creates can be changed as desired, based on the characteristics and positions of the suspended objects, to perform intelligent manipulations. With our hybrid IC / Microfluidic chip we have controlled the motion of individual cells in water, and droplets of water in oil.

Section 2. Theory of dielectric manipulation

Dielectrophoresis (DEP) is the movement of a particle in a non-uniform electric field due to the induced dipole moment of the particle relative to the surrounding medium (Pohl, 1978), as shown in Figure 2a. Dielectrophoresis is best implemented in microsystems that use large electric field gradients to manipulate particles at low Reynolds numbers; these are ideal for implementation with IC/Microfluidic chips. In this section, we discuss the theory and scaling of DEP for particle manipulation, as well as the fundamental limitations of DEP and specific considerations for DEP in biology.

2.1 Overview of Dielectrophoresis

The force on an electric dipole in an electric field is:

$$\vec{F}_{DEP} = (\vec{p} \cdot \nabla) \vec{E}, \quad (2.1)$$

where \vec{p} is the dipole moment of the particle relative to the surrounding medium, and \vec{E} is the external electric field. For a spherical particle of radius a with linear polarizability in an alternating (AC) applied electric field, the DEP force time averaged over an AC cycle is:

$$\vec{F}_{DEP} \propto a^3 \nabla E_{rms}^2 \quad (2.2)$$

where E_{rms} the root-mean-squared magnitude of the electric. Note that the DEP force does not act along electric field lines, but rather in the direction of the gradient of the electric field squared.

There are several important reasons to use AC fields for DEP. In a conductive medium, AC fields of sufficient frequency (> 10 kHz) do not suffer from ionic screening or electrode polarization: ions cannot move fast enough to screen the applied field. The movement of particles due to net charge (electrophoresis) will time average to zero in an AC field and electroosmotic flow of the double layer along liquid – solid boundaries is eliminated. Another benefit of AC fields is to reduce the voltage across the capacitive membrane of a cell, which we will discuss in Section 1.1.1.

The DEP force will act to move a particle in liquid against fluid drag. In microsystems, the inertia of a particle is very small compared to viscous forces: typical Reynolds numbers are $Re \sim 10^{-3}$. For low Reynolds number flow ($Re < 1$) the drag on a sphere is

$$\vec{F}_{drag} = -6\pi\eta a \vec{v}, \quad (2.3)$$

where η is the dynamic viscosity of the medium, a the radius of the sphere and v the velocity of the sphere relative to the medium. Low Reynolds number also allows us to ignore particle acceleration in our equations of motion, because particles typically reach terminal velocity after a few μs .

Solving the Laplace Equation for a conductive sphere in a conductive medium (Jones, 1995) we have:

$$\vec{F}_{DEP}(\omega) = 2\pi\epsilon_m a^3 CM(\omega) \nabla E_{rms}^2, \quad (2.4)$$

where ϵ_m is the medium permittivity, and $CM(\omega)$ is the Clausius-Mossotti factor, a relation between the frequency dependent complex permittivity of the particle and the medium.

$$CM(\omega) = \text{Re} \left[\frac{\hat{\epsilon}_p - \hat{\epsilon}_m}{\hat{\epsilon}_p + 2\hat{\epsilon}_m} \right], \quad (2.5)$$

where $\hat{\epsilon}_p$ and $\hat{\epsilon}_m$ are the complex permittivity of the particle and medium respectively.

The Clausius-Mossotti factor can vary between $CM(\omega) = -0.5$ and 1, with important physical implications, as shown in b. When $CM(\omega) < 0$, the fluid is more polarizable than the particle, and the particle is pushed toward the local minimum of the electric field. This is called negative DEP (nDEP). Positive DEP (pDEP) occurs when the particle is more polarizable than the fluid, $CM(\omega) > 0$, and the particle is pulled to the maximum of the electric field.

To determine the movement of a particle from Equations 2.3 and 2.4, we need to take a closer look at the polarization of a spherical particle relative to the surrounding medium. Particles and media with finite conductivity σ have a complex permittivity $\hat{\epsilon} = \epsilon - i\sigma/\omega$ that changes with frequency ω .

At low frequency, $CM(\omega)$ is dominated by conductivity, while at high frequency, permittivity dominates $CM(\omega)$. The relevant interfacial Maxwell-Wagner relaxation time is:

$$\tau_{mw} = \frac{\epsilon_p + 2\epsilon_m}{\sigma_p + 2\sigma_m}. \quad (2.6)$$

By controlling the electric field frequency, fluid conductivity, and electric field distribution, it is possible to trap a given particle with either nDEP or pDEP. To trap a particle with nDEP using planar electrodes, requires confinement in the perpendicular direction produced by a conductive coverslip, a physical boundary, or by gravitational force on the particle. The force due to gravity is $F_g = (4\pi/3)(\rho_p - \rho_m)a^3g \sim 0.1$ pN for a cell.

To manipulate biological cells using DEP, one must consider the capacitive cell membrane, which has a significant effect on the dielectric behavior. The effective complex permittivity $\hat{\epsilon}_p$ of the cell including a thin membrane (Jones, 1995) is:

$$\hat{\epsilon}_p = \frac{a\hat{C}_{mem}\hat{\epsilon}_{cyto}}{a\hat{C}_{mem} + \hat{\epsilon}_{cyto}}. \quad (2.7)$$

The complex membrane capacitance is $\hat{C}_{mem} = C_{mem} - iG_{mem}/\omega$, with C_{mem} the specific membrane capacitance, G_{mem} the specific membrane conductance, and $\hat{\epsilon}_{cyto}$ the complex permittivity of the cytoplasm. A plot of the calculated CM factor vs. frequency is shown in Figure 2b.

We now have equations that describe the DEP force on a particle or cell in a given electric field distribution. It is usually too complicated to find an analytic solution for the electric field pattern produced by an experimental electrode geometry. To find the field distributions, we run finite element modeling (FEM) simulations using either Comsol Multiphysics or Maxwell 3D (Ansoft), as is shown in Figure 2. After finding the electric field distribution (Figure 2d) for a given electrode geometry (Figure 2c), we extract the DEP force (Figure 2e) on a particle of interest and determine how fast the particle will move against fluid drag. Theory and FEM simulations described in this section were used to optimize the design of DEP microelectrodes in our IC/Microfluidic chips. Figure 2f shows the parameters used in our model to calculate the CM factor of mammalian cells.

2.2 *Scaling Relations of DEP Manipulation*

The smaller a DEP manipulation system is, the more powerfully it traps particles for a given voltage. Very closely spaced DEP pixels are no disadvantage: a particle can be captured

and smoothly translated across a fine DEP array by simultaneously operating a number of pixels, just like a display can show a large object moving across a screen by illuminating many pixels.

From Equation 2.4, the DEP force $\vec{F}_{DEP} \propto a^3 \vec{\nabla} E_{rms}^2$ is proportional to the volume of the particle and the gradient of the electric field squared. The magnitude ∇E_{rms}^2 can be estimated (Bahaj and Bailey, 1979) from the applied voltage V and the characteristic length l_e of the electrodes by $\nabla E_{rms}^2 \propto V^2 / l_e^3$. The maximum DEP manipulation force will be achieved when we match l_e and a , giving $F_{DEP}^{max} \propto V^2$, because the two cubic factors cancel. In water, with dielectric constant $81 \epsilon_0$, an applied voltage $V = 1V$ gives $F_{DEP}^{max} \sim 1$ nN. So DEP is a good way to apply pN to μ N forces to small objects in size microfluidic systems.

For microscopic electrodes, the DEP actuation voltage is limited by dielectric breakdown of the medium or the particle. A good dielectric can withstand fields of 10^7 to 10^8 V/m. In water, a voltage ~ 1 V can be applied across a 100 nm gap between two electrodes without risking dielectric breakdown; this produces a force $F_{DEP}^{max} \sim 1$ nN on a 100 nm particle of matched size. For larger electrode gaps l_e and particle sizes a , the dielectric breakdown limit permits greater voltages V and forces $F_{DEP}^{max} \propto V^2$. The voltage and force for large particles is eventually limited by practicality - it is difficult to switch voltages $> \sim 1$ kV at the MHz frequencies appropriate for DEP. As a consequence, the greatest DEP manipulation force that can be achieved is ~ 1 mN.

2.3 *Specific considerations for DEP in biology*

The fluidic environment in biocompatible microfluidic systems presents additional considerations and constraints for DEP manipulation that are considered in this section: heating of ionic solution that cells live in, electrohydrodynamic flow, and potentially harmful transmembrane voltages for cells.

The ionic solutions in which cells live have electrical conductivity ~ 1 S/m. The electric fields used to move cells lead to Joule heating by electric currents, which must be kept to a minimum to avoid harming the cells. The large surface to area ratio for microfluidic systems helps, by allowing this heat to flow away to the substrate.

Electrohydrodynamic (EHD) flow in a microfluidic system is caused by coupling between the density and the dielectric constant of the fluid. In a system with a temperature gradient, the density and dielectric constant vary spatially. In zero applied electric field, the thermal gradient causes convection - hot volumes of liquid expand and tend to rise against gravity, while colder volumes sink. When an electric field gradient is applied, the colder liquid volumes are also attracted to strong electric field locations creating EHD flow. For temperature gradients > 1 °C across a microfluidic chamber, the forces on a particle due to convective and EHD fluid flow can be the comparable or greater than DEP forces.

Minimizing the liquid ion concentration is an excellent way to avoid heating and EHD flow. Cells generally suffer no severe consequences from being suspended in low conductivity buffer, if the osmotic pressure is maintained by a non-ionic solution such as sucrose or mannitol. In the DEP experiments described below, we re-suspended cells in low conductivity ($\sim 10^{-3}$ S/m) solutions buffered with appropriate concentrations of non-ionic sugars to maintain osmolarity.

2.3.1 Transmembrane voltage induced by DEP

An important question in designing DEP hybrid IC/Microfluidics is whether the electric fields used to manipulate the cells interfere with inter-cellular activity. Ion pumps in a living mammalian cell maintain a transmembrane voltage of approximately 70 mV across the ~ 8 nm thick cell membrane. We expect only a small effect on cell physiology if the transmembrane voltage induced by the electric field used for DEP is less than ~ 10 mV. As the induced

transmembrane voltage increases past 100 mV, the electric field will cause electroporation of the cell membrane. Brief periods of electroporation can be useful within an experiment for delivering drugs, DNA, or RNA that would otherwise not be taken up by the cell (Olofsson et al., 2003). In most situations electroporation should be avoided to prevent damage to the cell. It is found that cells suffer minimal ill effects in electric fields < 100 kV/m at frequencies > 1 MHz (Voldman, 2001).

The maximum voltage induced across the membrane of a spherical cell in an external electric field is (Grosse and Schwan, 1992):

$$V_{tm} = \frac{1.5|E|a}{\sqrt{1 + (\omega\tau)^2}} \quad (2.8)$$

where the time constant to charge the cell membrane

$$\tau_{mem} = aC_{mem} \left(\frac{1}{\sigma_{cyto}} + \frac{1}{2\sigma_{medium}} \right), \quad (2.9)$$

is typically on the order of microseconds. Operating at MHz or higher frequencies reduces the voltage across the cell membrane. For cells with simulation parameters from Figure 2f, we find $\tau_{mem} = 1.4$ μ sec. For an applied electric field $E_{max} = 20$ kV/m, which is the magnitude of the field created by our IC, the transmembrane voltage falls from $V_{tm} = 140$ mV at 1 kHz to $V_{tm} < 20$ mV at 1 MHz, which is compatible with cell health.

2.4 Fundamental limitations of dielectrophoresis

2.4.1 Thermodynamic limits

To trap a particle against thermal fluctuations, the drop in energy of the particle as it enters the trap must be greater than $k_B T$, where k_B is Boltzmann's constant, and T is the temperature.

The radius r_{min} of smallest particle that can be trapped at room temperature is given by

$$2\pi\epsilon_m r_{\min}^3 E_{rms}^2 > k_B T, \quad (2.10)$$

with the maximum electric field E_{rms} set by dielectric breakdown of the particle and medium. In water, we find $r_{\min} \approx 1$ nm. As the trap volume decreases, restricting the phase space accessible to a trapped particle, entropy becomes an increasingly important consideration. Nonetheless, single protein molecules of radius ~ 5 nm have successfully been trapped with DEP (Holzel et al., 2005).

2.4.2 Cell manipulation limits

The maximum force on a cell and speed of motion that can be obtained using DEP are limited by the electric field induced across the cell membrane. We estimate the force $F_{DEP}^{\max} \approx 70$ pN for a maximum transmembrane voltage $V_{tm} = 100$ mV, using Equation 2.4 and parameters from Figure 2f. The maximum cell speed that we achieve with planar DEP electrodes in a hybrid IC/Microfluidic chip of the type described below is ~ 300 $\mu\text{m}/\text{sec}$. Higher cell speeds might be achieved by using higher frequencies that reduce the voltage across the cell membrane, allowing higher actuation voltages.

2.4.3 Droplet manipulation limits

An IC/Microfluidic chip can move pL droplets through an oil medium using positive DEP. The maximum speed is limited by the surface tension that prevents a single droplet from breaking into two or more smaller droplets. DEP requires a non-uniform electric field. If the field changes significantly across the diameter of the droplet, different portions of the droplet will be subject to different forces. If surface tension is insufficient to hold the droplet together, the droplet will split in two. A 17 μm diameter droplet was moved at speeds ~ 3 cm/sec

(Ahn et al., 2007). With careful electrode design and increased surface tension, droplets could be manipulated at higher speeds.

2.5 *Summary*

Dielectrophoresis is an excellent manipulation tool to position particles in microfluidic systems. DEP is able to move almost any particle, so long as a medium is chosen with a dielectric mismatch to the particle at a particular frequency. Cells suffer few ill effects from electric fields of magnitude less than 100 kV/m at frequencies higher than 1 MHz. Our calculations show that cells can be manipulated with DEP at speeds up to ~ 1 cm/sec and that particles of size ~ 5 nm can be captured and held against thermal fluctuations. Experiments with our IC/Microfluidic chip show that cells can be moved at speeds ~ 300 $\mu\text{m}/\text{sec}$.

Section 3. Materials

Our IC/Microfluidic chips are based on a general design that can be reprogrammed for many different uses. By using a standard CMOS process, our integrated circuit can be fabricated in a commercial foundry. The microfluidic system is built on top of the IC, at Harvard. The IC/Microfluidic chip is mounted on a standard 84-pin chip carrier, and connected to the computer using a printed circuit board that we design. Optical imaging of the motion of cells and droplets inside the IC/Microfluidic chamber are observed using a fluorescence microscope equipped with a digital video camera, recorded by the computer.

Imaging

1. Olympus BX microscope with an 20x objective (long working distance), a 5x objective (long working distance), and an X-Cite Series 120 light source.
2. ORCA-ER CCD camera (Hamamatsu).

3. Personal Computer (Dell)
4. Norpix Streampix software

Integrated circuit fabrication

1. Cadence Design Software
2. MOSIS 350 nm process, TSMC35_P2.

Microfluidics

1. Silicone gasket (Press-to-Seal; Invitrogen)
2. **Epoxy-based photoresist (SU-8; MicroChem)**
3. **Silicone elastomer kit (Sylgard 184; Dow Corning)**
4. **Sliver paste (SPI Supplies)**
5. **UV-curable adhesive (NOA-72; Norland)**

Electronics setup

1. DC power supply (Model PS2520a; Tektronix).
2. Function Generator (Model AFG3102; Tektronix).
3. Data Acquisition Board (Model PCI 6254; National Instruments).
4. Printed Circuit Board (E2 2-layer; PCB-Express).
5. Chip Carrier (84 JCC 0.460 x 0.460; Global Chip Materials).
6. Personal Computer (Dell).
7. Labview software (National Instruments).
8. Matlab software (Mathworks).

Reagents

1. D-Mannitol ACS Reagent (Sigma Aldrich).
2. Hexadecane 99% (Sigma Aldrich).

3. Fluorinert FC-40 (Sigma Aldrich).
4. Sodium dodecyl sulphate (SDS) surfactant (Sigma Aldrich).
5. Active Dry Yeast (Fleischmann's).
6. Yeast Peptone Dextrose agar (YPD) broth (Becton, Dickinson, and Company).
7. Magnetic beads (PCM-250; Kisker).
8. Phosphate buffered saline (PBS; Fisher Scientific).
9. Bovine serum albumin (BSA; Sigma Aldrich).
10. Bovine capillary endothelial cells (CRL-8659; ATCC).

Section 4. Methods

The purpose of an IC/Microfluidic system is to combine the power and flexibility of modern CMOS technology with the biocompatibility of a microfluidic system. The design of such a system requires careful consideration of each part and the ways in which they interact. The heart of the system is the IC. The IC electrically connects to the outside world (for electrical power and to send and receive data) through a printed circuit board. A microfluidic chamber immediately on top of the IC holds the biological samples that the IC will interact with. The inside of the microfluidic system is visualized by an optical microscope, equipped with a digital video camera. The operation of the IC is controlled by commands from a computer that also records images from the video camera. Custom software allows the user to manipulate objects inside the microfluidic chamber based on the video images of cells or objects inside.

This section describes the design process for the IC/Microfluidic chip and the implementation of the entire DEP manipulation system. The design flow that we followed, electric field simulations, process selection, circuit design, and circuit layout are discussed. We

also discuss the interface between the chip and the outside world, including packaging, microfluidics, and software for computer control.

4.1 IC/Microfluidic chip design

This section gives an overview of the IC/Microfluidic chip design process. Figure 3 shows the design flow that we followed to fabricate an IC/Microfluidic system. An excellent review of CMOS IC design is given by Weste and Harris (2005). Our IC contains a 128x256 array of pixels similar in geometry to a flat-panel display, shown in Fig. 4; each pixel creates a local RF electric field when it is activated. The pattern of activated pixels is determined by 128x256 SRAM memory - each pixel lies above a memory element. Finite-element simulations were used to confirm that the IC would produce appropriate electric field profiles for DEP inside the microfluidic chamber. An appropriate commercial IC process was chosen to match the simulation parameters. The coupling between the IC to the microfluidic chamber and the packaging requirements were kept in mind during the design process, to produce a successful hybrid IC/Microfluidic chip.

Before beginning detailed circuit design, we performed finite-element electrostatic simulations to model the electric field profiles produce by the pixel array, and the resulting DEP force on suspended objects inside the microfluidic chamber. These simulations were done to ensure that the IC/Microfluidic chip could trap and move cells. The calculations were executed with Maxwell 3D (Ansoft Inc) on an 8x8 array of square pixels with mirrored boundary conditions. For an 8 μm diameter cell above an electrode, the maximum electric field on a cell is ~ 50 kV/m, small enough to avoid harm the cell at frequencies > 1 MHz. The field gradient was large enough to generate a DEP force ~ 5 pN, sufficient to move a cell through the microfluidic chamber at speeds 10 to 100 $\mu\text{m}/\text{sec}$.

4.2 Process selection

The custom designed integrated circuit was fabricated in a commercial foundry. CMOS prototyping services for custom-designed ICs are available through the MOSIS (Metal Oxide Semiconductor Implementation Service) program originated by the National Science Foundation (NSF) - the area of a full-size wafer is divided into many chip designs, to reduce processing costs.

The pixel size and applied voltage are important parameters. The pixel area ($11 \times 11 \text{ mm}^2$) was chosen match the size of cells, to produce effective field gradients. For DEP, one would like to apply relatively large RF voltages. However, for logic, the voltage is reduced to avoid heating. As a compromise, we selected a $0.35 \text{ }\mu\text{m}$ gate length CMOS process with four metal layers and 5 V operating voltage, with $0.5 \text{ }\mu\text{m}$ gate length transistors, fabricated by Taiwan Semiconductor Manufacturing Company (TSMC) through MOSIS (TSMC35_P2 process).

An ideal DEP chip might have many small pixels to generate high-spatial-resolution electric field patterns. Larger areas of high field can be generated, simply by energizing nearby pixels, like a display. Small pixels are possible, as a result of the progress of the semiconductor industry. One should be able to produce DEP pixels with area as small as $1 \times 1 \text{ }\mu\text{m}^2$ using a 65 nm CMOS process. The minimum size of a pixel in our design is determined by the SRAM element below. Intel has demonstrated a $0.57 \text{ }\mu\text{m}^2$ SRAM cell using their 65 nm process (Zhang et al., 2005), compatible with a $1 \times 1 \text{ }\mu\text{m}^2$ pixel. In the 65 nm process, the operating voltage is usually reduced to $\sim 1 \text{ V}$ to minimize heating. This low voltage should produce sufficiently strong electric fields and field gradients for DEP, due to the short separation between pixels. The passivation thickness above the top metal layer must be reduced with the pixel size, so the field gradient used for DEP will penetrate into the microfluidic chamber.

4.3 Single pixel design

The DEP IC shown in Figure 4a, contains a 128x256 array of individually addressable pixels, as shown in Figure 4b. Beneath each pixel are circuit elements to control activation of its electric field. The circuit is shown as three circuit blocks in Figure 4c: 1) SRAM memory element to store the state of the pixel, 2) pass transistors that, depending on the state of the SRAM, allow either V_{pix} or the logical inverse (\bar{V}_{pix}) to be applied to the DEP electrode, and 3) pixel drive transistors to pull-up and pull-down the capacitive load of the pixel.

The voltage V_{pix} applied to the pixels is generated off chip. It is a 50% duty cycle square wave at a user selectable frequency, typically 1 MHz. Driving pixels with either V_{pix} or \bar{V}_{pix} rather than V_{pix} or ground provides advantages. The electric field between pixels held at V_{pix} and \bar{V}_{pix} time averages to zero so there is no electrophoresis for charged particles in the microfluidic system. In addition, the RMS electric field between V_{pix} and \bar{V}_{pix} is twice the magnitude of the RMS field between V_{pix} and ground, providing four times the DEP manipulation force. To pack pixels closely in the IC, the transistors were packed as densely as possible, within the design rules, with sufficient contact to the substrate and wells to avoid latch-up. To further conserve chip area, all PMOS transistors for pixels in a common word line shared an n-doping well.

4.4 IC design

The circuits and logic on the IC chip were designed using design rules, simulation parameters, and single transistor layout obtained from TSMC. IC simulation and layout were performed using Cadence Design Systems software. A pattern of energized pixels stored in the SRAM corresponds to an 'image' in a display. An image was loaded into the array by using bit control circuits and row control circuits (Figure 4b). Time dependent electric field patterns were created by displaying a series of stored images, like a movie. This approach is possible, because

the switching speed of the IC far exceeds the movie frame rate, giving ample time to load a new 'image' into the SRAM. The pixel addressing architecture is described in detail by Hunt et al. (2008).

4.5 *Microfluidics*

The microfluidic packaging scheme is shown in Figure 5a. We received raw IC dies from the TSMC foundry. All subsequent processing was done in the Center for Nanoscale Systems cleanroom at Harvard. We first mounted a die on a copper block for optimum heat transfer and wirebonded the IC to microfabricated leads next to the IC chip. Our initial microfluidic systems used standard microfluidic techniques to produce PDMS or SU-8 channel walls, as shown in Figure 5a. However, neither PDMS nor SU-8 channels are resealable, and PDMS is difficult to bond to rough or dirty substrates such as the copper block. To facilitate sealing and cleaning the microfluidic channel for multiple tests, we used hot-melt adhesive to form the microfluidic chamber walls. With hot-melt channel walls, we could easily remove the coverslip to clean the surface of the chip, or replace the entire channel.

4.6 *Mounting the integrated circuit*

Figure 5c shows a photograph of the DEP IC/Microfluidic experimental setup underneath an optical microscope, and Figure 5b shows a schematic diagram of the complete IC/Microfluidic chip system including the optical microscope, video camera and computer. The IC is mounted with silver paint on a removable 84-pin chip carrier, which fits against a copper block to allow thermal control of the microfluidic system for biocompatibility. The copper block may be cooled passively with forced air or water, or actively through a cooling system. A circuit board provides electrical connections to the chip. The pixel control lines can be connected to a microcomputer to input images of energized pixels for DEP manipulation, or they can be

independently contacted. The board also connects the V_{pix} RF signal from an external function generator to the chip, along with $\overline{V_{\text{pix}}}$, the logical inversion of V_{pix} , by an inverter on the circuit board. The circuit board also contains RC filters to provide protection against electrostatic discharge (ESD) and power regulation hardware. The board is mounted on a movable stage beneath an optical microscope that can be operated for fluorescence or bright field optical imaging. A digital video camera on the microscope transfers the images to the computer.

4.7 *Interface and software design*

Control signals for DEP are sent to the IC/Microfluidic chip by a 16 bit digital IO card (National Instruments PCI-6254 with LabVIEW software) mounted in a PC. The control lines are created and interpreted by LabVIEW (National Instruments). For future work, the IC/Microfluidic chip to computer interface could be simplified by implementing at low cost by using an on-board microcontroller and a USB port.

The state of the chip is controlled in a user interface written in MATLAB (MathWorks). In the MATLAB interface, the array of pixels on the chip is displayed as a 128x256 bitmap: white for pixels energized with V_{pix} , black for pixels set to $\overline{V_{\text{pix}}}$. The user can change any pixel in a region of interest, move blocks of energized pixels, or create standard patterns. The interface can also upload sequences of pictures, or movies, to the chip to produce repeating patterns across the chip.

A simple way to make a microfluidic chamber on the top surface of the IC is to use hot melt adhesive. A thin layer of adhesive was formed between two silanized glass slides on a hotplate, and the microfluidic chamber was cut out with a sharp hole punch (Harris UniCore, Pella Inc). Under a binocular dissecting microscope, we heated the chip to approximately 90 °C,

and bonded the patterned adhesive layer to the chip surface. With hot melt channel walls we could easily seal a microfluidic channel to even a surface with rough topography.

Fluid could be introduced in two ways: We could pipette a few μL of liquid to fill the microfluidic chamber and place a coverslip on top, or we could bond a coverslip with drilled holes to the top of the hot-melt channel and inject fluid with syringe pumps through the *via* holes. We have deliberately used microfluidic systems with very simple geometry - a chamber or channel - to demonstrate that our IC/Microfluidic chip can programmably control the position of many items at once. Conventional microfluidic systems require many channels, junctions, and fluid switches to accomplish the same function. But for an application, one may want to use a standard PDMS microfluidic system constructed on the top side of the coverslip to supply reagents, cells, and fluidic droplets to the chip through the *via* holes in a particular way.

4.8 *Conclusion*

This section describes the design and fabrication of a IC/Microfluidic chip system for DEP manipulation. Beginning with finite element simulations, we designed a two-dimensional array of DEP pixels, with displays an 'image' held by an SRAM memory underneath, and control electronics to load images into the SRAM. A microfluidic chamber was fabricated on the top surface of the chip, and cooled to regulate its temperature for experiments on cells. DEP manipulation was observed by an optical microscope equipped with a digital video camera, and controlled by a personal computer with custom software.

4.9 *Detailed Methods*

Design of Integrated Circuit

1. Cadence software package - design the hierarchical circuit schematic.

2. Run detailed electrical simulation of the designed circuit schematic.
3. Layout the mask layers for the hierarchical designs.
4. Test to ensure that all design rules are met.
5. Match the schematic to the layout.
6. Extract unintended circuit elements from the layout design and add to schematic.
7. Repeat electrical simulation, and repeat steps 2 through 6 until design parameters are met.
8. Submit the design to the foundry.
9. Receive ICs from foundry.
10. Test the ICs electrically.
11. Wirebond the IC to the chip carrier.
12. The chip carrier fits into a socket mounted on a custom printed circuit board that connects the chip to the data acquisition board

Adding microfluidic gasket to the IC

1. Cut the silicone gaskets to the same size as the IC.
2. Use a 1.5 mm hole punch to cut a hole in the center of the gasket.
3. Position gasket onto the IC under a stereo microscope.

Fabricating microfluidic systems on top of IC chips

In this method, an IC chip that has a small footprint (2 mm x 5 mm) is attached to a bigger Si/SiO₂ substrate for the subsequent fabrication. The fluidic structure is fabricated on top of the whole substrate.

1. Pattern electrical leads on a Si/SiO₂ substrate using standard microfabrication technique.
2. Glue an IC chip on the prepared substrate. For good electrical and thermal connection, silver-paste adhesives are recommended.

3. Pattern fluidic channels and ports. For example, epoxy-based resin (SU-8) can be spin-coated, patterned and cured to make sturdy structure.
4. Seal open channels. A thin layer of cured PDMS (polydimethylsiloxane) can be conformably placed or a thin glass slide can be glued with UV-curable adhesive.
5. Make electrical and fluidic connections.

Preparation of yeast Solution

1. Add active dry yeast to yeast broth.
2. Wait 3 hours.
3. Centrifuge yeast solution at 3,000 RPM for 30 sec.
4. Pipette out the yeast broth off of the top.
5. Replace broth with 100 mM mannitol solution.
6. Mix yeast and mannitol with a vortexer.
7. Pipette 3 μ l yeast into the gasket in the IC/Microfluidic device.
8. Place cover slip on top of rubber gasket.

Magnetic tagging of cells

1. Coat magnetic beads with GRGDSP using standard water-soluble carbodiimide chemistry (Daniel *et al.* 1998; Rowley *et al.* 1999).
2. Culture cells in the vendor recommend media and in presence of the magnetic beads (5 μ g/ml) for 24 hours at 37 °C.
3. Wash off unbound beads (3 times).
4. Trypsinize the cells and resuspend them in PBS buffer. Optionally, fix the cells by adding with 4% (w/v) paraformaldehyde solution.

5. Before introducing the cells to the microfluidic system, fill the channel with BSA (5% w/v) and incubate for 1 hr. This will reduce non-specific cell binding to channel walls.

Preparation of water droplets in oil

1. Mix Hexadecane, SDS, and water with green food coloring to make drop solution.
2. Mix in vortexer.
3. Pipette 1 μ L of FC-40 into the gasket in the IC/Microfluidic device.
4. Pipette 2 μ L drop solution into the gasket in the IC/Microfluidic device.
5. Place cover slip on top of rubber gasket

Manipulation of objects with the IC / microfluidic system

1. Power the IC/Microfluidic system with the DC power supply. The chip should draw 120 mA.
2. Write the pattern to be written to the chip on Matlab using a custom graphical interface.
3. Send the patterns written on Matlab to PCI 6254 digital acquisition board, which connects to the chip, using Labview.
4. Receive Patterns from the chip to ensure that that chip is operational.
5. Connect the RF source signal from the function generator to the printed circuit board.
6. Observe the motion of particles on the chip with the microscope.

Section 5. Examples

This section describes experimental demonstrations of our IC/Microfluidic system as a platform for the programmable positioning of single cells and pL droplets of liquids. The programmable positioning of cells and droplets provides a versatile technique for biomedical investigations - drug discovery, genetics, proteomics and beyond.

5.1 *Yeast manipulation with the IC/Microfluidic system*

The ability to independently position hundreds of single cells holds great promise for biological experiments. Positioning cells allows researchers to study cell-cell signaling, to assemble tissue from individual cells, and to control statistical numbers of individual cells for investigating stochastic processes (Lee et al., 2007).

The first demonstration of the manipulation of individual cells with the IC/Microfluidic system was performed on yeast. Single yeast cells were captured by energizing a few pixels of the IC/Microfluidic chip with V_{pix} , while all of the other pixels were driven with its inverse \bar{V}_{pix} . By changing which pixels were energized, individual cells were moved from the top of one pixel to the top of a neighbouring pixel at speeds $\sim 30 \mu\text{m}/\text{sec}$. By energizing non-neighbouring pixels it was possible to move yeast cells at speeds up to $\sim 300 \mu\text{m}/\text{sec}$.

Yeast cells were cultured overnight in YPD broth (BD Inc.) at 37°C . The conductivity of the broth was approximately $1 \text{ S}/\text{m}$ as measured by an Orion 116 conductivity meter (Thermoelectron Inc). The yeast were re-suspended in a mannitol buffer, with a conductivity of $100 \mu\text{S}/\text{m}$, to reduce the effects of heating and EHD flow in the strong electric fields produced by the DEP chip. A $5 \mu\text{L}$ volume of yeast cells in mannitol was pipetted into the microfluidic chamber on the chip.

The IC/Microfluidic chip can simultaneously control the motion of two different cells. Figure 6a shows a time sequence of an individual yeast cell and a mammalian cell (a rat alveolar macrophage) being trapped and moved. In the sequence of three panels, the yeast and mammalian cell were first moved upwards (red arrows) then joined together. Experiments with the system showed that it was possible to move an individual cell along an arbitrary path by energizing a sequence of pixels. It was also possible to separate two cells that are close together,

or to bring two cells together that were initially apart together. These motions were defined by a user, who observed the resulting cell motion through the microscope. Because there are no channels in the microfluidic chamber, a wide variety of motions can be programmed.

Rat alveolar macrophages were prepared by the Bioimaging Lab at Harvard School of Public Health. The cells were obtained by bronchoalveolar lavage and suspended in a low conductivity buffer, 0.1 M sucrose, to avoid heating and EHD flow. Residual ions brought the conductivity of the sucrose buffer to 100 $\mu\text{S}/\text{M}$.

By appropriately addressing the pixel array, we could simultaneously trap and move hundreds of individual cells. Figure 6b shows yeast cells that have been moved to form an image programmed into the DEP array - the pixels were energized in a bitmap to spell "Lab on a Chip". To make the pattern, yeast cells in mannitol were pipetted onto the chip surface. As the cells settled due to gravity, they were attracted to the local maxima in the electric field produced by the pattern of energized pixel electrodes on the chip surface. The image in Figure 6b was taken after all of the cells had settled to the surface of the chip, roughly 10 minutes after introducing the yeast suspension.

5.2 *Droplet manipulation*

Microfluidic systems that are capable of manipulating droplets can serve as a platform for programmable, automated chemistry. Droplets of chemicals from reservoirs along the edge of the chip can be mixed together to perform a wide variety of biochemical assays, from DNA sequencing to transcription (Whitesides, 2006; Ahn et al., 2006). Controlling the motion of individual droplets is a major accomplishment for our IC/Microfluidic system. Water droplets with volumes ~ 1 pL to ~ 1 nL were programmably manipulated. The IC/Microfluidic system can be used to carry out biochemical tests rapidly, with pL volumes of liquid, on many samples at the

same time. In addition, drug tests on a single cell can be conducted by merging a droplet containing a chemical dose with a second droplet that contains a cell.

To prepare droplets for manipulation, a mixture of hexadecane, water, and sodium dodecyl sulphate (SDS) surfactant, was shaken using a vortexer. A thin layer of fluorocarbon oil was pipetted onto the surface of the chip and then the suspension of water droplets in hexane was added to the microfluidic channel. The difference in density n among the three liquids resulted in water droplets ($n = 1 \text{ g/cm}^3$) that were pinched between a layer of dense fluorocarbon oil ($n = 2.4 \text{ g/cm}^3$) and less dense hexadecane ($n = 0.8 \text{ gm/cm}^3$).

The resulting multilayer liquid provided very little resistance to the translation of droplets in a plane above the surface of the chip. The droplets were not in contact with the chip surface so it was not necessary to overcome contact line hysteresis to move the droplets. In addition, droplet manipulation was insensitive to the surface treatment and hydrophobicity of the chip. Water droplets in hexadecane alone wetted and stuck to the polyimide surface of the chip despite surface pretreatment schemes including silinization and evaporated fluorocarbon oil.

Figure 6c shows a sequence of frames that demonstrate how the IC/Microfluidic chip can be used to split, move, and combine droplets of water in an oil medium using positive DEP; the energized pixels are highlighted in white. By sequentially changing which pixels are energized, water droplets may be translated through the oil medium. The first four panels in Figure 6c show how one can split a single large drop into two smaller droplets. First, a pair of pixels was energized at the top and bottom ends of the drop. These two pairs were then pulled apart, elongating the drop in the second panel. The drop was stretched farther in the third panel, causing it to split into two smaller droplets, shown in the fourth panel. The resulting droplets could be independently moved as demonstrated in the fifth and sixth panel. Finally the two

droplets were jointed into one, by bringing them into contact in panels seven and eight. The splitting, translation, and recombining of pL aqueous droplets, controlled by a computer, is a powerful application of our IC/Microfluidic system.

Section 6. Future directions for IC/Microfluidic systems

6.1 Summary

An IC/Microfluidic chip combines the biocompatibility of microfluidics with the built-in logic, programmability, and sensitivity of ICs. We designed, built and tested an IC for moving dielectric particles such as cells and water droplets using DEP. The IC was built in a commercial foundry and a microfluidic chamber was then fabricated on its top surface. The chip contains a two dimensional array of 128x256 individually addressable $11 \times 11 \mu\text{m}^2$ pixels that covers a $1.4 \times 2.8 \text{ mm}^2$ area. When energized, a pixel creates a localized electric field above, to trap a cell, or a droplet of water in oil. This is done by applying an RF voltage V_{pix} of magnitude 5 V at a frequency up to 1.8 MHz. By shifting the location of energized pixels, the array can trap and move cells along programmable paths through the microfluidic chamber.

The true strength of the IC/Microfluidic chip is its programmability. The chip can move a droplet, cell, or other dielectric particle to any location in inside the two-dimensional microfluidic chamber, and many objects can be independently manipulated at the same time. The chip is a general-purpose device that can be programmed for use in many different applications, unlike a conventional microfluidic system, which is composed of a network of channels. Their adaptability allows IC/Microfluidic chips to be programmed to react in real time to the outcome of a test. Parallel tests can be performed at the same time on the large

128x256 pixels (32,768 pixels) that may be updated in less than a second. The DEP cell velocities are typically $\sim 10 \mu\text{m}/\text{sec}$, and can be as large as $\sim 300 \mu\text{m}/\text{sec}$.

IC/Microfluidic chips are scalable into larger and more complex systems. Larger arrays with more pixels are possible, because current CMOS technology can produce ICs capable of addressing millions of pixels over a 1 cm^2 area. It is also possible to add new functionality to the IC/Microfluidic chip, including electronic sensors, temperature control, or magnetic manipulation capabilities built inside the IC. Hybrid IC/Microfluidic chips have the advantages of programmability, scalability, and versatility over their standard microfluidic counterparts.

6.2 *Applications of the DEP manipulator*

A wide range of biomedical investigations require automated, parallel manipulation of small chemical volumes and single cells. Drug discovery, genetic sequencing and synthesis, cell sorting, and single cell gene expression studies all rely on rapid, small volume manipulation. IC/Microfluidic chips provide a versatile platform for programmable and adaptable manipulation that matches the demands of these diverse fields (Lee et al., 2007; Hunt et al. 2008).

Besides developing new applications for current DEP manipulator chips, it is interesting to develop next-generation chips that offer stronger manipulation forces or higher spatial resolution. Stronger DEP forces can be achieved with a DEP chip designed for a high voltage CMOS process to achieve manipulation speeds much faster than our 5V chip. Higher spatial resolution DEP manipulator chips with pixel sizes $\sim 1 \times 1 \mu\text{m}^2$, could be constructed using a 45 nm or 65 nm CMOS process. These could be used to position smaller objects into complex patterns with submicron resolution.

6.3 *Future directions for IC/Microfluidic systems*

IC/Microfluidic chips have the potential to make a major impact on biomedical research. With ICs becoming more powerful each year and microfluidics entering the commercial arena, IC/Microfluidic chips can benefit from advances in both industries.

Programmable systems go beyond common microfluidic devices that serve a single purpose with a fixed channel geometry. IC/Microfluidic systems can be used as a general-purpose microfluidic microprocessor for performing a wide variety of microfluidic assays. With appropriate fluid inputs and outputs, droplets of reagents could be combined, heated, mixed, split, observed optically or with NMR, and sent to an output all within an IC/Microfluidic system. In addition, with the massive parallelism available in modern ICs, hundreds or even thousands of reactions could be controlled simultaneously, far surpassing the throughput of even the fastest pipetting robot. Our IC/Microfluidic DEP manipulator chip, capable of moving pL chemical volumes and statistical numbers of individual cells demonstrates only a small portion of the possibilities for IC/Microfluidic systems.

Acknowledgements

We thank Prof Donhee Ham for advice on integrated-circuit design and the use of his chip design software, and Dr Rick Rogers and Dr Rosalinda Sepulveda at the Harvard School of Public Health for providing mammalian cells. This work was supported by the National Cancer Institute through the MIT-Harvard Center for Nanotechnology Excellence.

References

- Ahn, K., Kerbage, C., Hunt, T.P., Westervelt, R.M., Link, D.R., and Weitz, D.A. (2006). Dielectrophoretic manipulation of drops for high-speed microfluidic sorting devices. *Appl. Phys. Lett.* *88*, 024104.
- Bahaj, A.S. and Bailey, A.G. (1979). Dielectrophoresis of microscopic particles. *J. Phys. D* *12*, L109.
- Ballan, H. and Declercq, M. (1999). *High Voltage Devices and Circuits in Standard CMOS Technologies*, (Dordrecht, Kluwer).
- Blazej, R.G., Kumaresan, P., and Mathies, R.A. (2006). Microfabricated bioprocessor for integrated nanoliter-scale Sanger DNA sequencing. *PNAS* *103*, 7240-7245.
- Chin, C.D., Linder, V., and Sia, S.K. (2007). Lab-on-a-chip devices for global health: Past studies and future opportunities. *Lab Chip*. *7*, 41, and refs. therein.
- Current, K., Yuk, K., McConaghy, C., Gascoyne, P., Schwartz, J., Vykoukal, J., and Andrews, C. (2005). A high-voltage CMOS VLSI programmable fluidic processor chip. *IEEE Symposium on VLSI Circuits Digest*, 72.
- Daniel, S.G., Westling, M. E., Moss, M. S. and Kanagy, B.D. (1998). FastTag Nucleic Acid Labeling System: a versatile method for incorporating haptens, fluorochromes and affinity ligands into DNA, RNA and oligonucleotides. *Biotechniques*, *24*, 484.
- DeBusschere, B.D. and Kovacs, G.T.A. (2001). Portable cell-based biosensor system using integrated CMOS cell-cartridges. *Biosensors & Bioelectronics* *16*, 543.
- Duffy, D.C., Mc Donald, J.C., Schueller, O.J., Whitesides, G.M. (1998). Rapid prototyping of microfluidic systems in poly(dimethylsiloxane). *Anal. Chem.* *70*, 4974.
- Eversmann, B., Jenkner, M., Hofmann, F., Paulus, C., Brederlow, R., Holzapfl, Fromherz, B.P., Merz, M., Brenner, M., Schreiter, M., Gabl, R., Plehnert, K., Steinhauser, M., Eckstein, G., Schmitt-Landsiedel, D., and Thewes, R. (2003). Cell-lab on a chip: a CMOS-based microsystem for culturing and monitoring cells. *J. Solid-State Circuits* *38*, 2306.
- Facer, G.R., Notterman, D.A., and Sohn, L. (2001). Dielectric spectroscopy for bioanalysis: From 40 Hz to 26.5 GHz in a microfabricated wave guide. *Appl. Phys. Lett.* *78*, 996.
- Green, N.G. and Morgan H. (1997). Dielectrophoretic investigations of sub-micrometre latex spheres. *J. Phys. D: Appl. Phys.* *30*, 11 L 41.
- Green, N.G., Morgan, H., and Milner, J.J. (1997). Manipulation and trapping of sub-micron bioparticles using dielectrophoresis. *J. Biochem. Biophys. Methods* *35*, 89.

- Grosse, C. and Schwan, H. (1992). Cellular membrane potentials induced by alternating fields. *Biophysical J.* *63*,1632.
- Hölzel, R., Calander, N., Chiragwandi, Z., Willander, M., and Bier, F. (2005). Trapping single molecules by dielectrophoresis. *Phys. Rev. Lett.* *95*, 128102.
- Hunt T.P., Lee H., and Westervelt R.M. (2004). Addressable micropost array for the dielectrophoretic manipulation of particles in fluid. *Appl. Phys. Lett.* *85*, 6421.
- Hunt T.P., Issadore, D., Westervelt R.M. (2008). Integrated circuit/microfluidic chip to programmably trap and move cells and droplets with dielectrophoresis. *Lab Chip* *8*, 81-87.
- Jones T.B. (1995). *Electromechanics of Particles*, (Cambridge, Cambridge Univ. Press).
- Lee, J., Moon, H., Fowler, J., Schoellhammer, T., and Kim, C.J. (2002). Electrowetting and electrowetting-on-dielectric for microscale liquid handling. *Sens. Actuators A* *95*, 259.
- Lee, H. Microelectronic / microfluidic hybrid system for the manipulation of biological cells, (2005). PhD dissertation, Harvard University.
- Lee, H., Liu, Y., Alsberg, E, Ingber, D.E., Westervelt R.M., and Ham D. (2005). An IC/microfluidic hybrid microsystem for 2D magnetic manipulation of individual biological cells. *Digest of Technical Papers, IEEE International Solid-State Circuits Conference 1*, 80.
- Lee, H., Liu, Y., Westervelt, R.M., and Ham, D., (2006). IC/microfluidic hybrid system for magnetic manipulation of biological cells. *IEEE J. Solid-State Circuits* *41*, 1471.
- Lee, H. Ham, D. and Westervelt, R.M. eds. (2007). *CMOS Biotechnology* (New York, Springer).
- Lee, H., Liu, Y., Ham, D., Westervelt, R.M. (2007). Integrated cell manipulation system—CMOS/microfluidic hybrid. *Lab. Chip* *7*, 331.
- Maguire, Y., Chuang, I.L., Zhang, Z., and Gershenfeld, N. (2007). Ultra-small-sample molecular structure detection using microslot waveguide nuclear spin resonance. *PNAS* *104*, 9198.
- Manaresi, N., Romani, A., Medoro, G., Altomare, L., Leonardi, A. Tartagni, M., and Guerrieri, R. (2003). A CMOS chip for individual cell manipulation and detection. *IEEE J. Solid-State Circuits* *30*, 2297.
- Olofsson, J., Nolkranz, K., Ryttsén, F., Lambie, B., Weber, S.G., and Orwar, O. (2003). Single-cell electroporation. *Curr. Opin. Biotechnol.* *14*, 29.
- Pohl, H. and Crane, J., (1971). Dielectrophoresis of cells. *Biophysical Journal* *11*, 711.

- Pohl, H.A., Dielectrophoresis (1978). (Cambridge, Cambridge Univ. Press).
- Pollack, M.G., Shendorov, A.D., and Fair, R.B. Electrowetting-based actuation of droplets for integrated microfluidics. (2002). *Lab Chip* 2, 1, 96.
- Psaltis, D., Quake, S.R., and Yang, C. (2006). Developing optofluidic technology through the fusion of microfluidics and optics. *Nature* 27, 442.
- Rowley, J.A., Madlambayan, G. and Mooney, D.J. (1999). Alginate hydrogels as synthetic extracellular matrix materials. *Biomaterials* 20, 45.
- Squires, T., Quake, S.R. (2005). Microfluidics: fluid physics at the nanoliter scale. *Phys. Rev. Lett.* 77, 977.
- Stone, H.A., Stroock, A.D., and Ajdari, A. (2004). Engineering flows in small devices. *Annual Reviews of Fluid Mechanics* 36, 381, and refs. therein.
- Tabeling, P. (2005). *Introduction to Microfluidics* (Oxford, Oxford Univ. Press), and references therein.
- Thewes, R., Hofmann, F., Frey, A., Holzapfl, B., Schienle, M., Paulus C., Schindler, P., Eckstein, G., Kassel, C., Stanzel, M., Hintsche, R., Nebling, E., Albers, J., Hassman, J., Schulein, J., Goemann, W., Gumbrecht, W. (2002). Sensor arrays for fully-electronic DNA detection on CMOS. Sensor arrays for fully-electronic DNA detection on CMOS. *Digest of Technical Papers, 2002 IEEE International Solid-State Circuits Conference* 1, 350.
- Thorsen, T., Maerkl, S.J., and Quake, S.R. (2002). Microfluidic large-scale integration. *Science* 298, 580.
- Voldman, J. (2001). A microfabricated dielectrophoretic trapping array for cell-based biological assays, Ph.D. dissertation, MIT.
- Vykoukal, J., Schwartz, A., Becker, F.F., and Gascoyne, P.R.C. (2001). A programmable dielectrophoretic fluid processor for droplet-based chemistry. *Micro Total Analysis Systems*, 72.
- Weste, N. and Harris, D. (2005). *CMOS VLSI Design: A Circuits and Systems Perspective*, (Addison Wesley).
- Whitesides, G.M. (2006). The origins and the future of microfluidics. *Nature* 442, 368.
- Whitesides, G.M., Ostuni, E., Takayama, S., Jiang X., and Ingber, D. (2001). Soft lithography in biology and biochemistry. *Annual Review of Biomedical Engineering* 3, 335, and refs. therein.

Wood, D.K., Oh, S.H., Lee, S.H., and Soh, H.T. (2005). High-bandwidth radio frequency Coulter Counter. *Appl. Phys. Lett.* *87*, 184106.

Yong, L., Sun, N., Lee, H., Weissleder, R., Ham, D. (2008). CMOS mini nuclear magnetic resonance system and its application for biomolecular sensing. *IEEE Int. Solid State Circuits Conf. (ISSCC) Digest of Tech. Papers*, p. 140.

Zhang, K., Bhattacharya, U., Chen, Z., Hamzaoglu, F., Murray D., Vallepalli, N, Wang, Y., and Bohr, M. (2005). SRAM design on 65-nm CMOS technology with dynamic sleep transistor for leakage reduction. *J. Solid-State Circuits* *40*, 895.

Figure Captions

Figure 1 a) Scanning electron micrographs of channels in PDMS by the Whitesides Group (Duffy et al., 1998). b) A microfluidic chip to measure protein interactions by the Quake Group. The colored lines pneumatically actuate valves that act as gates and pumps, which drive reagent solutions through the uncolored channels (Squires et al., 2005). c) The Intel Dual Core microprocessor (Intel). d) A magnetic-manipulation IC/Microfluidic system designed in our lab (Lee et al., 2006).

Figure 2 a) An illustration of dielectrophoresis. If $\epsilon_p > \epsilon_m$, the object is pulled into the maximum of the electric field gradient - this is called positive DEP. If $\epsilon_p < \epsilon_m$, it is negative DEP, and the object is repelled from the maximum field gradient. b) Calculated frequency dependence of the CM factor for mammalian cells. c) Electric potential of two pixels energized to 5V d) Resulting electric field magnitude 4 μm above the surface of the chip. e) Components of the DEP force parallel to the chip surface acting on the center of an 8 μm diameter cell in the microfluidic channel according to Equation 2.5. f) Model parameters used to calculate the DEP force on mammalian cells in the above figures.

Figure 3 IC/Microfluidic System Design Flow

Figure 4 a) Microscope image of the IC/Microfluidic system integrated circuit, b) Block diagram of the integrated circuit. Pixels energized with V_{pix} produce a local electric field in the microfluidic channel and apply DEP force to particles in the channel. c) Pixel Schematic. The circuit consists of three major parts, an SRAM memory element, pass transistors, and pull-up and pull-down transistors to drive the pixel. The state of the SRAM selects a pass transistor that sends V_{pix} or \bar{V}_{pix} to the pixel-drive transistors.

Figure 5 a) Schematic diagram of an IC/Microfluidic system. The IC is located beneath the microfluidic channel where electric and magnetic fields from the IC can interact with cells or chemical droplets in the microfluidic channels. b) Block diagram of the IC/Microfluidic system including a fluid loader, computer control, and an optical microscope with a digital camera that

feeds images to the computer, creating a system that can be completely closed loop, or receive inputs from a human user. c) A photograph of the IC/Microfluidic system embedded in its experimental apparatus.

Figure 6 a) Time sequence of yeast and rat alveolar macrophages trapped and moved with DEP using the IC/Microfluidic chip. Pixels on the chip were energized to independently move the two cells and then bring them together. The maximum speed of a yeast cell was approximately 30 $\mu\text{m}/\text{sec}$. b) The words "Lab on a Chip" spelled out by hundreds of yeast cells patterned by DEP. Pixels across the array were energized attracting cells toward the local maximum of the electric field. c) Splitting, moving, and combining water droplets in oil with DEP using the IC/Microfluidic chip. This time sequence shows a droplet of colored water between a layer of fluorocarbon oil below and hydrocarbon oil above. Pixels energized with V_{pix} in each frame are highlighted in white.

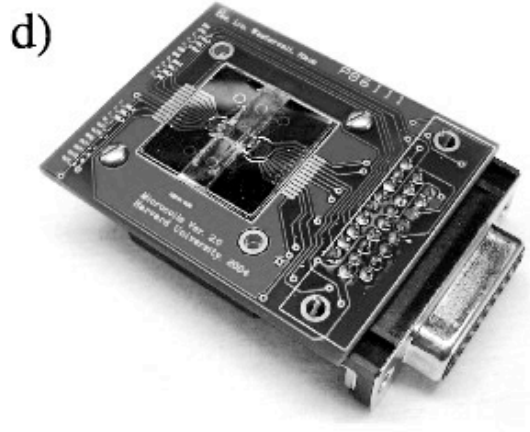
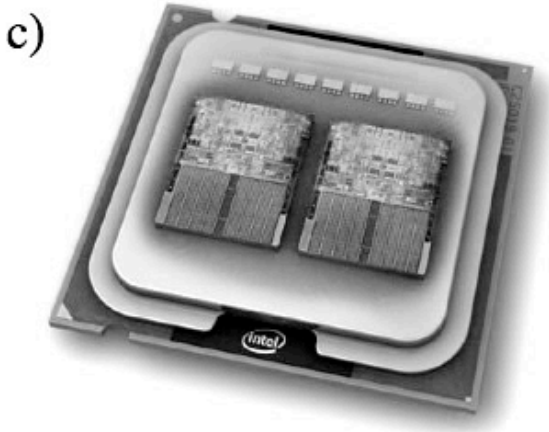
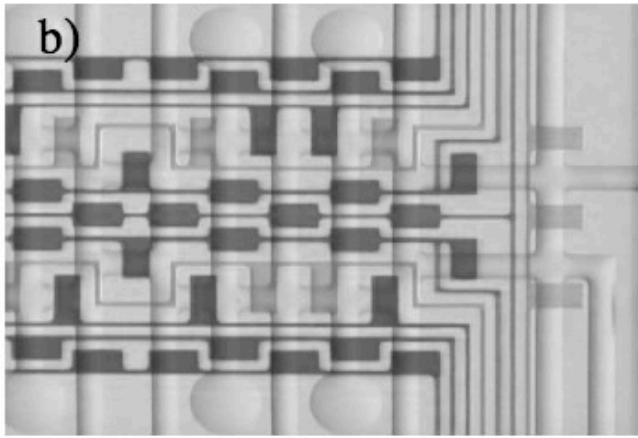
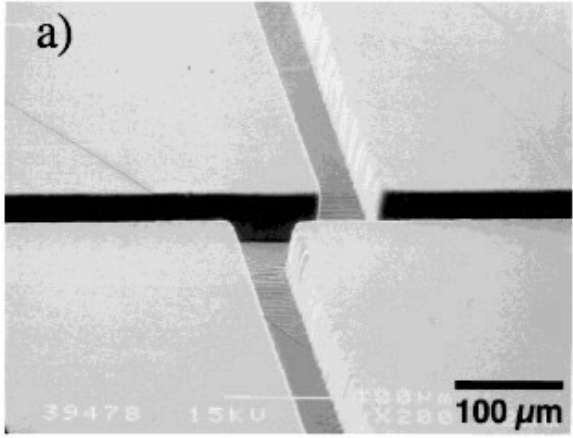


Figure 1

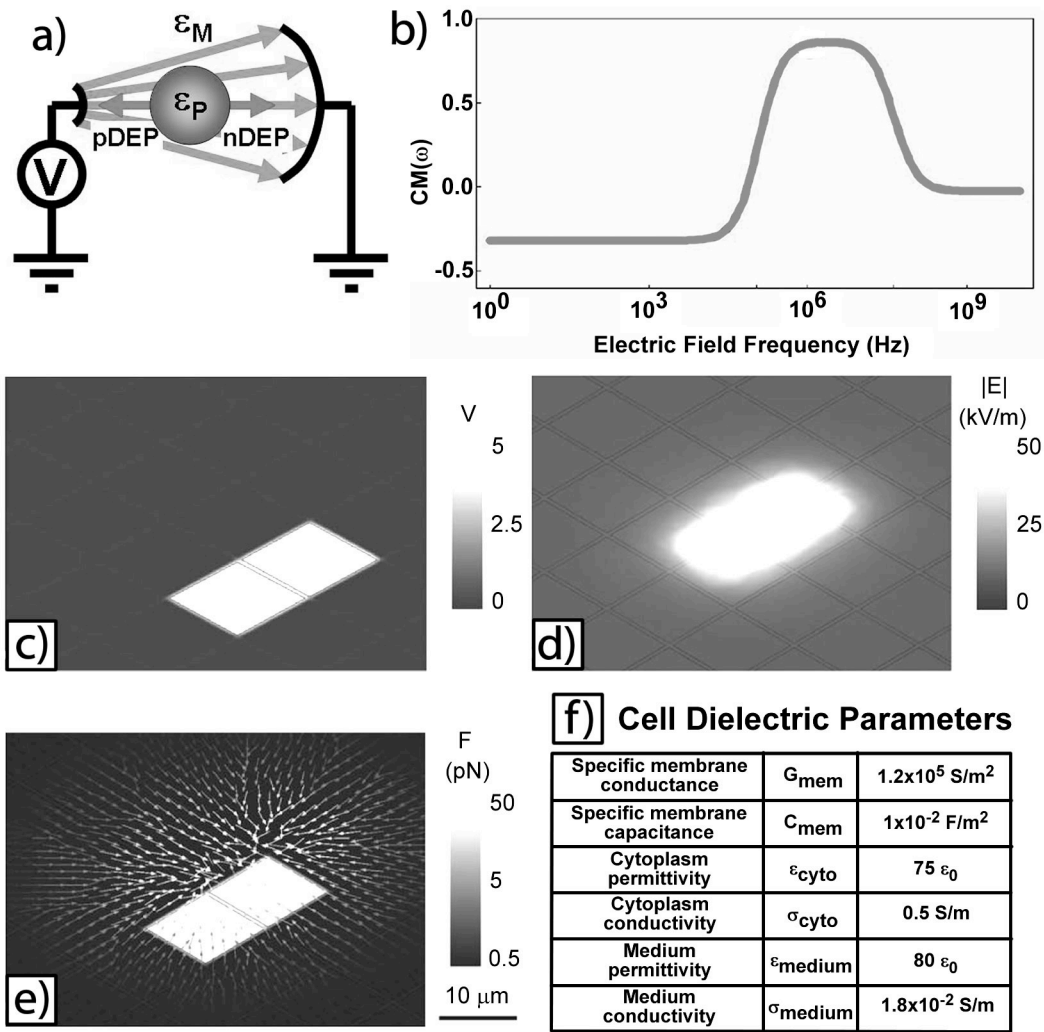


Figure 2

IC / Microfluidic System Design Flow

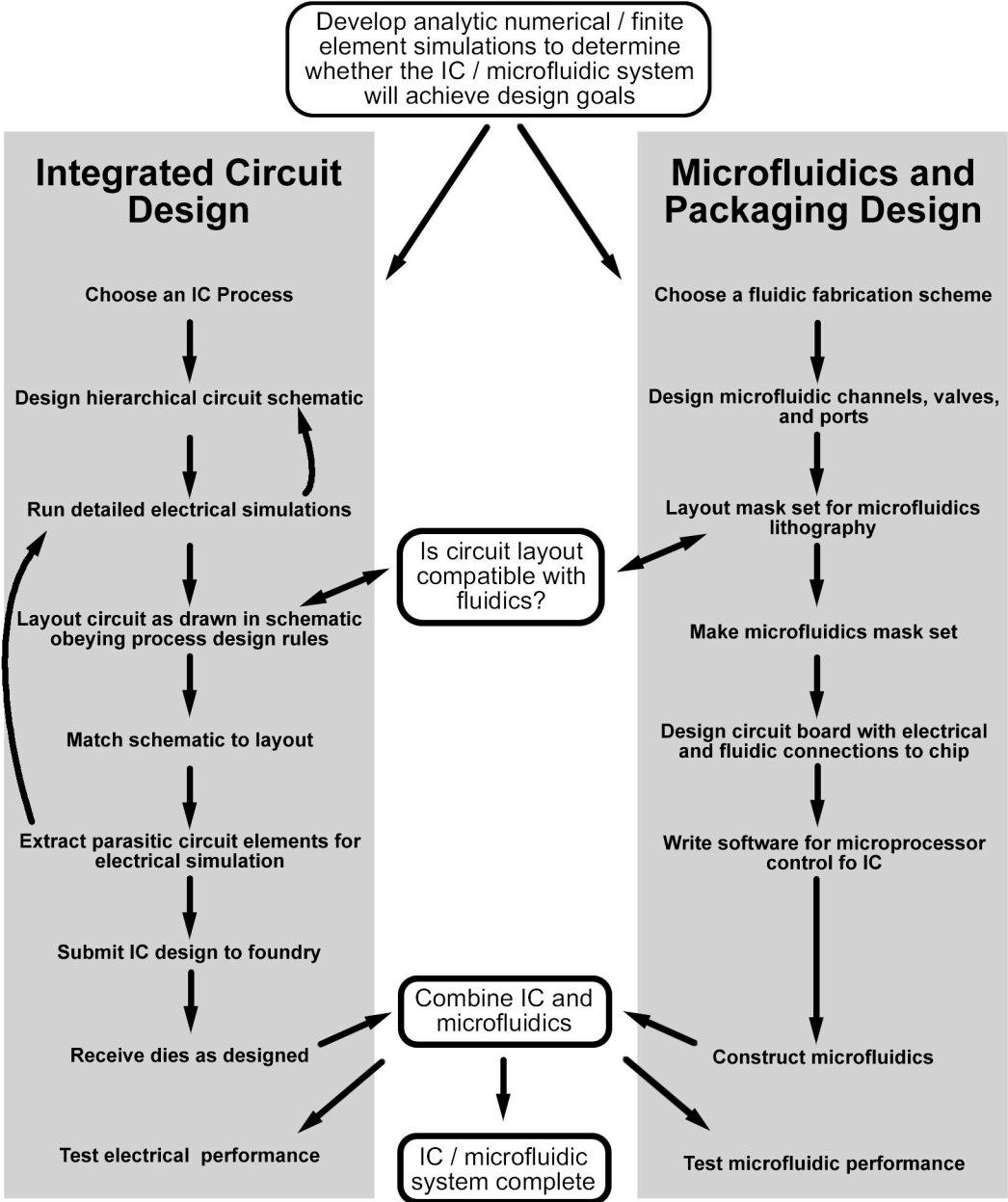


Figure 3

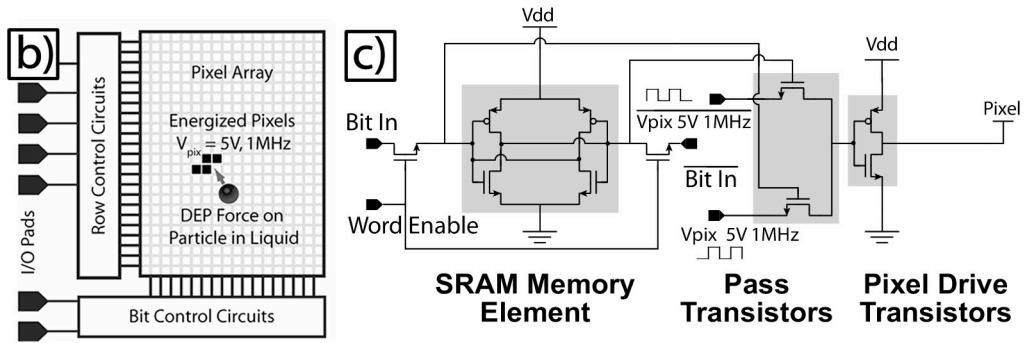
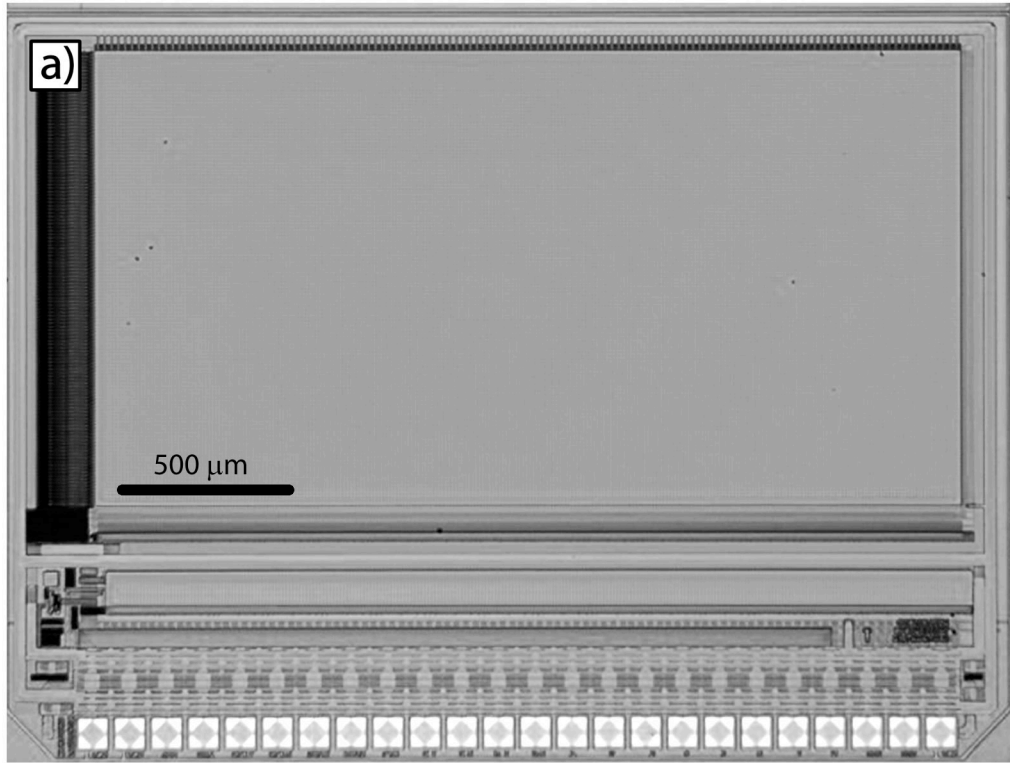


Figure 4

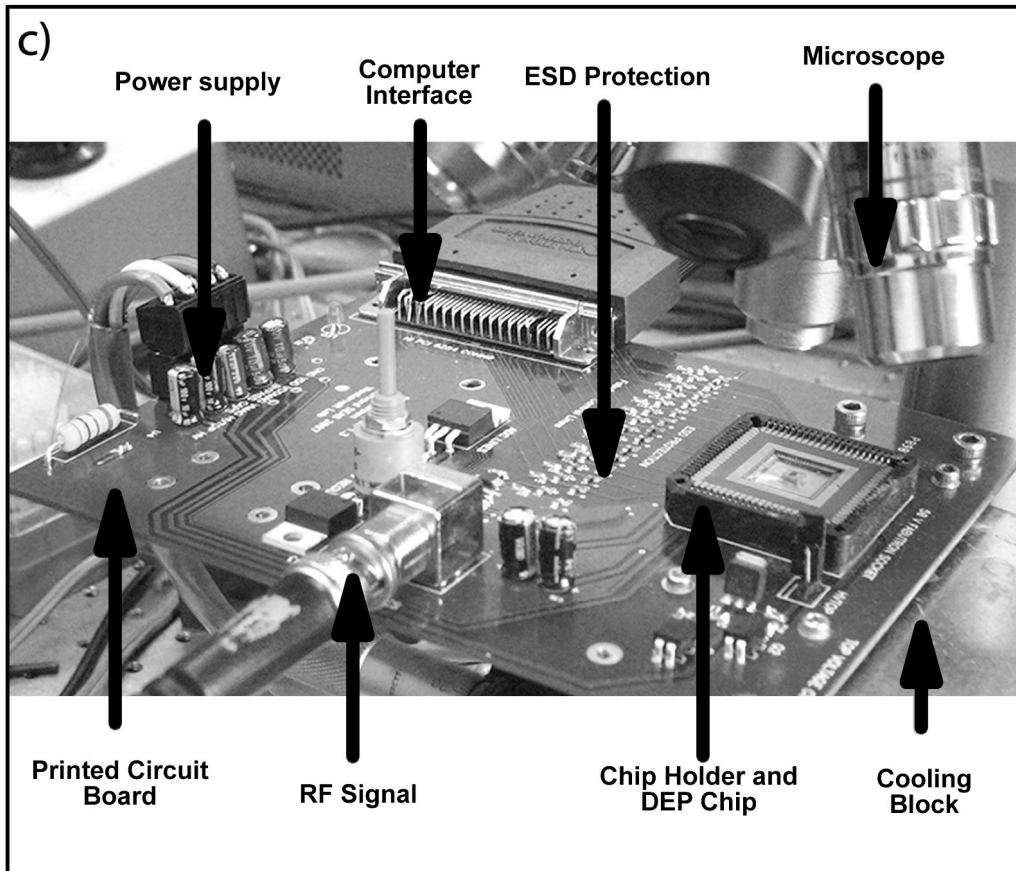
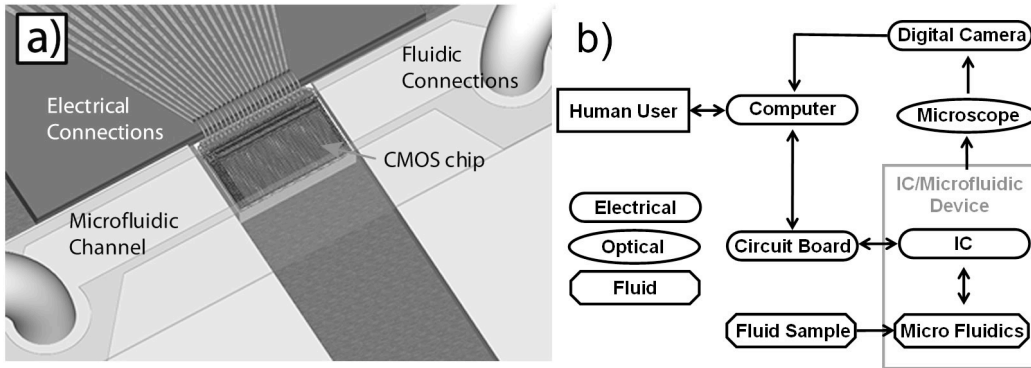


Figure 5

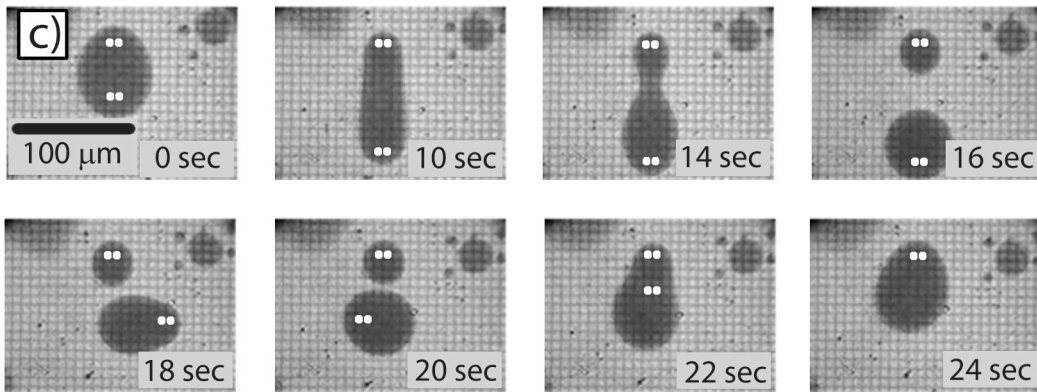
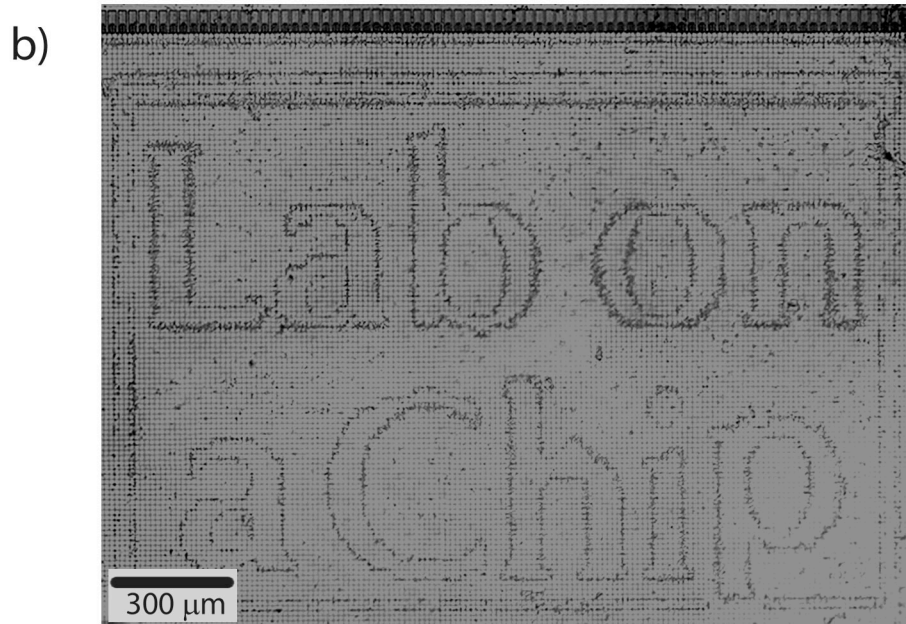
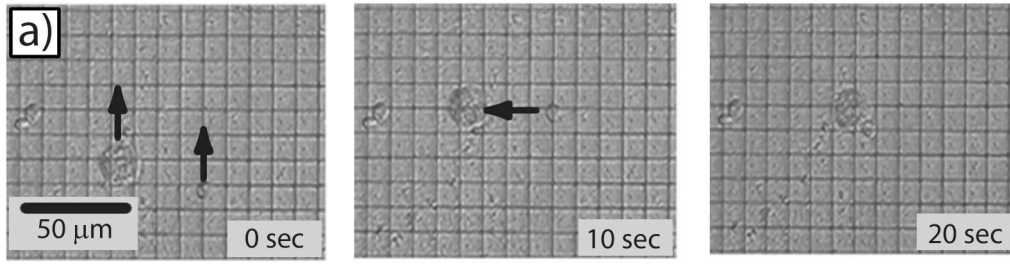


Figure 6